The Journal of Experimental Biology 209, 748-765
Published by The Company of Biologists 2006
doi:10.1242/jeb.02051

Anatomically diverse butterfly scales all produce structural colours by coherent scattering

Richard O. Prum[1,*], Tim Quinn[2] and Rodolfo H. Torres[3]

[1]*Department of Ecology and Evolutionary Biology, and Peabody Museum of Natural History, Yale University, PO Box 208105, New Haven, Connecticut 06250, USA,* [2]*Department of Ecology and Evolutionary Biology and* [3]*Department of Mathematics, University of Kansas, Lawrence, KS 66045, USA*

*Author for correspondence (e-mail: richard.prum@yale.edu)

Accepted 20 December 2005

Summary

The structural colours of butterflies and moths (Lepidoptera) have been attributed to a diversity of physical mechanisms, including multilayer interference, diffraction, Bragg scattering, Tyndall scattering and Rayleigh scattering. We used fibre optic spectrophotometry, transmission electron microscopy (TEM) and 2D Fourier analysis to investigate the physical mechanisms of structural colour production in twelve lepidopteran species from four families, representing all of the previously proposed anatomical and optical classes of butterfly nanostructure. The 2D Fourier analyses of TEMs of colour producing butterfly scales document that all species are appropriately nanostructured to produce visible colours by coherent scattering, i.e. differential interference and reinforcement of scattered, visible wavelengths. Previously hypothesized to produce a blue colour by incoherent, Tyndall scattering, the scales of *Papilio zalmoxis* are not appropriately nanostructured for incoherent scattering. Rather, available data indicate that the blue of *P. zalmoxis* is a fluorescent pigmentary colour. Despite their nanoscale anatomical diversity, all structurally coloured butterfly scales share a single fundamental physical color production mechanism – coherent scattering. Recognition of this commonality provides a new perspective on how the nanostructure and optical properties of structurally coloured butterfly scales evolved and diversified among and within lepidopteran clades.

Key words: coherent scattering, structural colours, Fourier analysis, photonics, Lepidoptera, *Callophrys, Celastrina, Morpho, Mitoura, Papilio, Parides, Parrhasius, Troides, Urania.*

Introduction

The pigmentary colours of organisms are produced by differential absorption of visible wavelengths by pigment molecules (Fox, 1976). In contrast, the structural colours of organisms are produced by the physical interactions of light waves with biological nanostructures that vary in refractive index (Fox, 1976; Nassau, 1983; Parker, 1999; Srinivasarao, 1999; Prum and Torres, 2003a). Structural colours are an important component of the phenotype of many animals (Fox, 1976; Herring, 1994; Parker, 1999) and even some plants (Lee, 1997).

The physical mechanisms of structural colour production are usually described as being quite diverse (Fox, 1976; Nassau, 1983; Parker, 1999; Srinivasarao, 1999). A short list of commonly proposed mechanisms includes interference, diffraction, reinforcement, multilayer reflection, Bragg scattering, Rayleigh scattering, Tyndall scattering, Mie scattering, and more. One major reason for this apparent mechanistic diversity is that the traditional physical tools used to analyze structural colour production vary with the anatomy of the colour producing nanostructure, i.e. its laminar, crystal-like, or quasi-ordered organization (Prum and Torres, 2003a). However, the diversity of physical tools for a diversity of anatomical organizations has reinforced the notion that the physical mechanisms of color production are actually diverse as well. Traditionally, the physical mechanism associated with each anatomy has been assigned based on the mathematical method that has been used to analyze it. In this way, the biological literature has drawn on a specific intellectual tradition within optics of naming optical phenomena according to the historical, experimental conditions in which each was first described (e.g. Hecht, 1987). While convenient in optical physics, this intellectual perspective has overshadowed the appreciation of the overwhelming physical, mechanistic commonality that underlyies the optical function of most colour-producing biological nanostructures, despite their anatomical diversity.

Until recently, the biological literature on structural colour has obscured the most fundamental physical distinction among all mechanisms of structural colour production: incoherent *vs*

coherent scattering (e.g. Prum and Torres, 2003a; Prum and Torres, 2003b; Prum and Torres, 2004). Incoherent scattering is the differential scattering of light wavelengths by individual scatterers, and it is determined by the size, shape and refractive index of individual scatterers without regard to the phase relationships among multiple waves scattered by different objects (van de Hulst, 1981; Bohren and Huffman, 1983). In contrast, coherent scattering is differential scattering of light wavelengths from multiple objects, and it is determined by the phase relationships among scattered light waves (Huxley, 1968; Benedek, 1971; Land, 1972; Joannopoulos et al., 1995; Prum and Torres, 2003a; Prum and Torres, 2003b).

Incoherent light scattering requires that the light scattering objects are spatially independent, or randomly distributed over spatial scales of the same order of magnitude in size as the wavelengths of visible light. Spatial independence insures that the phase relationships among scattered waves are random, and can thus be ignored in the calculations of light scattering (Bohren and Huffman, 1983). Rayleigh and Tyndall scattering (Young, 1982; Prum and Torres, 2003a) describe incoherent scattering by particles the size of visible light or smaller, and they predict the production of short wavelength hues: blue, violet and ultraviolet.

Coherent scattering occurs when spatial variation in refractive index is periodic, resulting in predictable phase relationships among light waves scattered by different objects. Interference, reinforcement, diffraction, multilayer and thin-film reflection, and Bragg scattering are all forms of coherent scattering. A wide variety of different nanostructures with periodic spatial variation in refractive index over one, two or three dimensions, can result in coherent scattering.

Unlike incoherent scattering, coherent scattering can produce the phenomenon of iridescence – a prominent change in hue or brilliance with angle of observation or illumination – because changes in angle of observation and illumination may affect the phase relationships among the scattered waves that determine the hue. Consequently, since 1923, iridescence has often been inaccurately synonymized with coherent scattering (Mason, 1923), leading to the indiscriminant assignment of noniridescent blue structural colours to incoherent, Rayleigh or Tyndall scattering (Fox, 1976; Nassau, 1983; Herring, 1994). Recently, however, it has been shown that a previously unappreciated class of nanostructures, called quasiordered arrays, can produce noniridescent or weakly iridescent colours by coherent scattering alone (Prum et al., 1998; Prum et al., 1999a; Prum et al., 1999b; Prum and Torres, 2003a; Prum and Torres, 2003b; Prum and Torres, 2004). To advance the understanding of the physics and evolution of organismal structural colours, it is important to conduct comparative analyses of a diversity nanostructures, and to investigate what they share in common and how they differ.

Butterfly structural colours

Structural colours are an important component of the phenotype of many butterflies and a few diurnal moths (Fig. 1) (Ghiradella, 1991; Nijhout, 1991; Ghiradella, 1998; Parker, 1999; Vukusic and Sambles, 2000; Vukusic et al., 2000a). Structural colours of butterflies can function in many ways from aposematic communication among species to mate choice within species (e.g. Sweeney et al., 2003).

The structural colours of butterflies (Lepidoptera) are produced by periodic nanostructures of chitin and air in the scales of the wings (Ghiradella, 1991; Vukusic and Sambles, 2000; Vukusic et al., 2000a). Lepidopteran wing scales are arranged in a series of rows like shingles on a house (Figs 2, 3). Typical butterfly scales have a complex structure that is characterized by a series of longitudinal ridges that are spanned by cross ribs, which sit on a basal lamellae that is supported by columnar trabeculae (Downey and Allyn, 1975; Ghiradella, 1985; Ghiradella, 1989; Ghiradella, 1991; Ghiradella, 1998). Structurally coloured scales exhibit a wide diversity of specializations of the ridges, cross ribs and complex compartmentalization of the basal region below 'windows' formed by the ridges and cross ribs on the surface of the scale (reviewed in Ghiradella, 1974; Ghiradella, 1985; Ghiradella, 1991; Ghiradella, 1998; Vukusic and Sambles, 2000; Vukusic et al., 2000a).

The structural colours of butterfly wing scales are a premier example of apparent diversity in physical mechanisms of colour production. A recently proposed 'optical classification' of structurally coloured butterfly scales recognizes three main types of scales, based on a combination of both anatomical and mechanistic/physical criteria (Vukusic et al., 2000a). Type I scales include those with surface lamellae (or laminae) that function by multilayer interference (Ghiradella, 1998; Vukusic et al., 2000a) and/or by diffraction (e.g. Kinoshita et al., 2002; Yoshioka and Kinoshita, 2003). Type II scales include those with internal structures that function by multilayer interference. Type III scales include (a) internal nanostructures forming 3D lattices that function by Bragg scattering or diffraction, and (b) internal nanostructures that produce colour by incoherent Rayleigh/Tyndall scattering.

The fundamental difficulty with this classification is that anatomical criteria, i.e. superficial *vs* interior position within the scale, or laminar *vs* crystal-like organization, have been combined with various mechanistic/physical criteria, i.e. multilayer interference *vs* diffraction *vs* Rayleigh/Tyndall scattering. This classification proposes that the anatomical distinction between multilayer interference scales (Types I and II) and all other mechanisms (Type III) is more fundamental than the distinction between diffraction (Type IIIa) and Rayleigh/Tyndall scattering (Type IIIb). Anatomical variations on incoherent scattering are lumped with incoherent scattering, and separated from other types of coherent scattering despite the fundamental mechanistic differences. This conceptual obfuscation reflects a long intellectual tradition in the study of biological structural colour production going back at least to 1976, when Fox discussed Tyndall scattering and diffraction in one chapter and iridescent colours in another (Fox, 1976).

To explore the physical commonalties shared among anatomically diverse butterfly nanostructures, we examined

Fig. 1. Photographs of the butterfly species examined. Uraniidae: (A) *Urania fulgens*; Papilionidae: (B) *Papilio ulysses*, (C) *Papilio zalmoxis*, (D) *Parides sesostris*, (E) *Troides brookiana*, (F) *Troides urvillianus*, (G) *Troides priamus priamus* (phenotypically similar to the green *T. p. hecuba* examined); Lycaenidae: (H) *Celastrina ladon*, (I) *Callophrys dumetorum*, (J) *Mitoura gryneus* and (K) *Parrhasius m-album* (very similar and closely related to the *P. moctezuma* examined); Nymphalidae: (L) *Morpho aega*. Photos are of upper wing surfaces, except for *Callophrys dumetorum* (I) and *Mitoura gryneus* (J), which are underwing surfaces. Not to scale. Specimens courtesy of the Yale Peabody Museum of Natural History Department of Entomology.

thirteen different colors of structurally coloured scales from twelve species of Lepidoptera from four different families (Fig. 1; Table 1) that represent all of the previously recognized types of colour producing butterfly scales. These species were chosen because the structural colours of these species (or their very close relatives) have previously been studied and attributed to a diversity of physical mechanisms including multilayer interference, diffraction, Bragg scattering and Tyndall scattering (Ghiradella, 1974; Huxley, 1975; Morris, 1975; Allyn and Downey, 1976; Ghiradella and Radigan, 1976; Huxley, 1976; Ghiradella, 1985; Ghiradella, 1989; Ghiradella, 1991; Vukusic et al., 1999; Vukusic and Sambles, 2000; Vukusic et al., 2000a; Vukusic et al., 2001a; Kinoshita et al., 2002; Yoshioka and Kinoshita, 2003). We use the two dimensional (2D) Fourier transform of transmission electron micrographs of the colour producing biological nanostructures

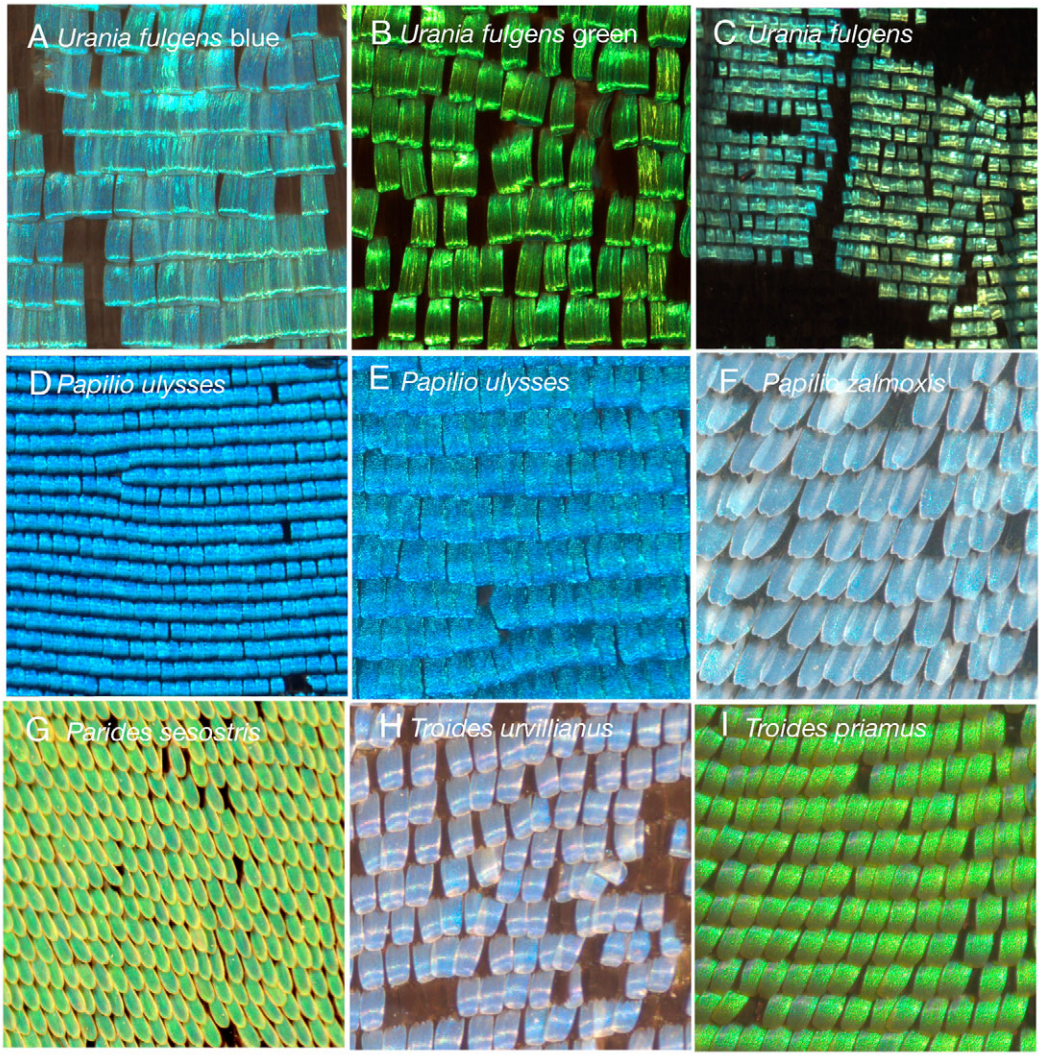

Fig. 2. Light microscope photographs of the structurally coloured scales of a sample of the Lepidoptera examined. (A) *Urania fulgens* blue, (B) *Urania fulgens* green, (C) *Urania fulgens* showing the transition between blue and green patches, (D,E) *Papilio ulysses,* (F) *Papilio zalmoxis*, (G) *Parides sesostris*, (H) *Troides urvillianus*, (I) *Troides priamus*. All images at 63×, except C (20×) and D (40×). Classification of species examined is given in Table 1.

in butterfly scales to analyze the periodicity of spatial variation in refractive index and predict the reflectance spectrum produced by coherent scattering from these scales (Prum et al., 1998; Prum et al., 1999a; Prum et al., 1999b; Prum and Torres, 2003a; Prum and Torres, 2003b).

Our results document that this diversity of scales from all major structural and optical classes all function by coherent scattering. Further, we conclude that the blue colour of the scales of *Papilio zalmoxis,* previously hypothesized to be produced by incoherent Tyndall scattering (Huxley, 1976) is likely to be a pigmentary colour. The conceptual unification of all lepidopteran structural colour production as variation of a single physical mechanism will allow us to understand better the evolution of the diversity of anatomy and the optical properties that have fascinated all previous workers in the field.

Materials and methods

Species sampled and microscopy

The butterfly and moth scales examined include 13 different colours from twelve species in four lepidopteran families (see Table 1 for details and taxonomic authorities). Blue and green samples were taken from the same individual *Urania fulgens* (Uraniidae). Blue and green samples were taken from individuals of two sister species differentiated on different Australopapuan islands: the blue *Troides urvillianus* from Guadacanal and the green *Troides priamus hecuba* from the Kai, or Key, Islands (Papilionidae).

Small (<cm^2) samples of structural coloured butterfly wings were taken from specimens in the Snow Entomology Collection of the University of Kansas Museum of Natural History (Table 1). Most species were selected specifically because their nanostructure and structural colours have been

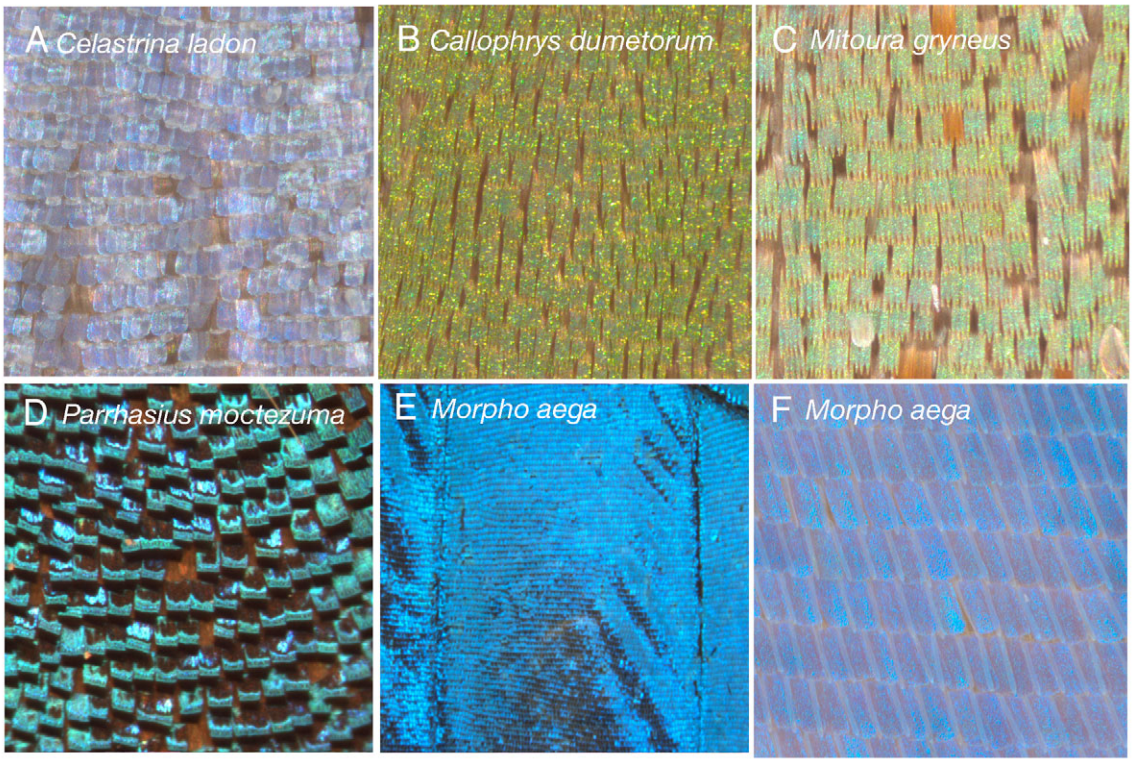

Fig. 3. Light microscope photographs of the structurally coloured scales of a sample of the Lepidoptera examined. (A) *Celastrina ladon*, (B) *Callophrys dumetorum*, (C) *Mitoura gryneus*, (D) *Parrhasius moctezuma* and (E,F) *Morpho aega.* All images at 63×, except D (70×) and E (7.5×). Classification of species examined is given in Table 1.

Table 1. *Classification and localities of the species examined*

Taxon	Locality
Family Uraniidae (swallowtail moths)	
Subfamily Uraniinae	
Urania fulgens (Walker 1854)	Peru: Moyobamba Province
Family Papilionidae (swallowtail butterflies)	
Subfamily Papilioninae	
Papilio ulysses autocylus C. & R. Felder 1865	West Irian: Arfak Mountains
Papilio zalmoxis Hewiston 1864	Central African Republic: Bangui
Parides sesostris (Cramer 1979)	Brazil
Troides brookiana (Wallace 1855)	Unknown
Troides urvillianus Guérin-Mené 1838	Guadalcanal
Troides priamus hecuba Röber 1891	Kai (or Key) Islands
Family Lycaenidae (blues and coppers)	
Subfamily Polyommantinae	
Celastrina ladon	Kansas: Douglas County
Subfamily Theclinae	
Callophrys dumetorum (Boisduval 1852)	Unknown
Mitoura gryneus (Hübner 1819)	Kansas: Douglas County
Parrhasius moctezuma Clench 1971	Mexico: San Luis Potosi
Family Nymphalidae (admirals, fritillaries and brush-footed butterflies)	
Subfamily Morphinae	
Morpho aega Hübner 1822	Peru: Huanuco

described before (Ghiradella, 1974; Huxley, 1975; Morris, 1975; Ghiradella and Radigan, 1976; Huxley, 1976; Ghiradella, 1985; Ghiradella, 1989; Ghiradella, 1991; Vukusic et al., 1999; Vukusic and Sambles, 2000; Vukusic et al., 2000a; Vukusic et al., 2001a). Images in Fig. 1 are of specimens of conspecific or closely related species from the Yale Peabody Museum Entomology collection.

For transmission electron microscopy (TEM), specimens were soaked in 100% ethanol for 24 h, and infiltrated with EMBED 812 (Electron Microscopy Services, Hatfield, PA, USA) for 24 h. Sections were cut approximately 100 nm thick, and stained with uranyl acetate and lead citrate and placed on formvar coated grids. Specimens were viewed with a JEOL EXII (JEOL USA, Peabody, MA, USA) transmission electron microscope. Digital micrographs were taken at various magnifications with a Soft-Imaging Megaview II CCD camera (Lakewood, CO, USA; 1024×1200 pixels).

Reflectance spectra

Reflectance spectra of the butterfly specimens were measured with an Ocean Optics S2000 (Dunedin, FL, USA) fibre optic spectrophotometer and an Ocean Optics deuterium-halogen light source, and a Dell laptop computer. The S2000 provides 2048 data points between 178 and 879 nm. Reflectance was measured using normal incident light at 6 mm distance from a 3 mm^2 patch of the integument with a 300 μs integration time. Reflectance was calculated in a standard fashion (e.g. Prum et al., 1999a) using an Ocean Optics Spectralon white standard.

2D Fourier analysis

Coherent scattering of visible wavelengths is a consequence of nanoscale spatial periodicity in refractive index of a tissue. Following a theory of corneal transparency by Benedek (1971), we developed a method of using the discrete Fourier 2D transform to analyze the periodicity and optical properties of structural coloured tissue, and predict its reflectance spectrum due to coherent scattering (Prum et al., 1998; Prum et al., 1999a; Prum et al., 1999b; Prum et al., 2003; Prum and Torres, 2003b; Prum and Torres, 2003a; Prum and Torres, 2004).

The digital TEM micrographs of structurally coloured butterfly scales were analyzed using the matrix algebra program MATLAB (Version 6.2; www.mathworks.com) on a Macintosh computer. The scale of each image (nm/pixel) was calculated from the number of pixels in the scale bar of the micrograph. A 1024 $pixel^2$ portion of each array was selected from each image for analysis.

The average refractive index of the tissue in each image was estimated by generating a two-partition histogram of image darkness (i.e. the distribution of darker and lighter pixels). The frequency distribution of darker and lighter pixels was used to estimate the relative frequency of chitin and air in the tissue, and to calculate a weighted average refractive index for the tissue using refractive indices of 1.54 for chitin and 1 for air.

The Fourier transforms were calculated with the 2D Fast Fourier Transform (FFT2) algorithm (Briggs and Henson, 1995). We then calculated the 2D Fourier power spectrum, or the distribution of the squares of the Fourier coefficients. The 2D Fourier power spectra were expressed in spatial frequency (nm^{-1}) by dividing the initial spatial frequency values by the length of the matrix (pixels in the matrix×nm/pixel). The 2D Fourier power spectrum resolves the spatial variation in refractive index in the tissue into its periodic components in any direction from a given point (Fig. 6).

We produced predicted reflectance spectra for each specimen based on the 2D Fourier power spectra of a sample of TEM micrographs, the image scales, and the estimated values of the average refractive index in the tissues. First, a radial average of the % power was calculated for concentric radial bins, or annuli, of the power spectrum corresponding to fifty 10 nm wide wavelength intervals between 300 and 800 nm (covering the entire insect visible spectrum). The radial average power values were expressed in % visible Fourier power by normalizing the total power values across all potentially visible spatial frequencies (between 300 and 800 nm) to 1. The inverse of the spatial frequency averages for each wavelength were then multiplied by twice the estimated average refractive index of the medium and expressed in terms of wavelength (nm). A composite predicted reflectance spectra was produced by averaging the normalized predicted spectra from a sample of TEM images. In *Troides brookiana,* the predicted reflectance spectrum was calculated from the averages of 30° wide sections (i.e. 'pie slices') of the power spectra directly above the origin to avoid the confounding effects of the horizontal periodic structure of the multiple ridges (Fig. 6E). For other laminar nanostructures, comparisons were made between spectral predictions based on radial average of the entire power spectrum or small radial sections (or pie slices) of the power spectrum around the peaks. Because these power spectrum peaks include an overwhelming proportion of the total Fourier power, results from the two different analyses were extremely similar.

Results

Colour and spectrophotometry

The butterfly and moth scales examined include 13 colours from 11 species in four lepidopteran families (Tables 1, 2). These samples exhibited a wide variety of violet, blue and green structural colours and iridescent effects (Fig. 1). All of the structurally coloured scales examined were from the upper surfaces of the wings, except for *Callophrys dumetorum* and *Mitoura gryneus*, which were from the underwing surfaces (Fig. 1I,J). The structurally coloured scales of all species were arranged in parallel rows like shingles on a house, but the scales of different species varied extensively in whether they were flat or curved, highly shiny or metallic, nearly translucent or exhibiting sparkling, opalescent highlights of colour (Figs 2, 3).

Reflectance spectra of almost all species revealed unimodal peak hues that correspond closely to the observed colours (Figs 8, 9, blue). *Celastrina ladon* showed the smallest wavelength peak reflectance of 375 nm (Fig. 9C), and *Troides*

Table 2. *Summary of results for the 13 different samples of structurally colored butterfly scales examined*

Family *Species*	Observed color	Observed peak hue (nm)	Fourier predicted peak hue (nm)	Prediction error (nm)	TEM figures	Reflectance and predicted spectra
Uraniidae						
Urania fulgens	Blue	473	470	3	4A,B	8A
Urania fulgens	Green	560	590	30	4C	8B
Papilionidae						
Papilio ulysses autocylus	Blue	475	510	35	4D,E	8C
Papilio zalmoxis	Blue	480	740	260	4F,G	8D
Parides sesostris	Green	545	530	15	4H–J	8E
Troides brookiana	Green	490	510	20	4K,L	8F
Troides urvillianus	Blue	475	470	5	5A,B	9A
Troides priamus hecuba	Green	585	560	25	5C	9B
Lycaenidae						
Celastrina ladon	Violet	375	390	15	5D	9C
Callophrys dumetorum	Green	555	570	15	5E,F	9D
Mitoura gryneus	Green	545	520	25	5G	9E
Parrhasius moctezuma	Blue	495	520	25	5H	9F
Nymphalidae						
Morpho aega	Blue	500	480	20	5I	9G

priamus exhibited the longest peak wavelength of 585 nm (Fig. 9B). The reflectance spectrum of the lycaenids in the sample (*Celastrina ladon, Callophrys dumetorum, Mitoura gryneus* and *Parrhasius moctezuma*) all showed blue or green peaks with gradually increasing reflectance above 600 nm (Fig. 9C–F). These long wavelength reflectances are very similar among species and may be produced by some unidentified pigment.

Anatomy and nanostructure

With the exception of *Parrhasius moctezuma* (Lycaenidae), the anatomy of the colour producing scales of the species analyzed here, or their very close relatives, have been previously described with SEM, TEM or both (Ghiradella, 1974; Morris, 1975; Allyn and Downey, 1976; Ghiradella and Radigan, 1976; Ghiradella, 1985; Ghiradella, 1989; Ghiradella, 1991; Ghiradella, 1998; Vukusic et al., 1999; Vukusic and Sambles, 2000; Vukusic et al., 2000a; Vukusic et al., 2001a; Kinoshita et al., 2002; Yoshioka and Kinoshita, 2003).

Troides brookiana (Papilionidae) and *Morpho aega* (Nymphalidae) are characterized by complex, multilayer, laminar structures on longitudinal scale ridges (Type I of Vukusic et al., 2000a). *Troides brookiana* has a unique arrangement of laminar outgrowths, or microribs, of neighboring ridges that create a series of tubular air channels between the laminae of each ridge and the laminae of adjacent ridges (Fig. 4K,L). In *Morpho aega*, the colour producing nanostructures are complex 'pine tree-shaped' elaborations of the longitudinal scale ridges (Fig. 5I). As reported previously from *Morpho didius* (Vukusic et al., 1999; Yoshioka and Kinoshita, 2003), *Morpho aega* has a second class of 'glass scales' with only a few longitudinal ridges that are widely spaced on a thin basal lamina. These glass scales function to diffuse the blue colour of the underlying scales (Vukusic et al., 1999; Yoshioka and Kinoshita, 2003).

Urania fulgens (Uraniidae), *Papilio ulysses, Troides urvillianus, Troides priamus* (Papilionidae), *Celastrina ladon* and *Parrhasius moctezuma* (Lycaenidae) are characterized by a generally laminar nanostructures of air cavities within the body of the scales (Type II of Vukusic et al., 2000a). In *Urania fulgens,* the arrays of air spaces are entirely flat (Fig. 4A–C). However, the scales of *Papilio ulysses* (Fig. 4D,E) and *Parrhasius moctezuma* (Fig. 5H) have concavities in the upper surfaces of the scales that distort the multilayers of rectangular air cavities in the scale. Where adjacent concavities meet beneath scale ridges, the multilayers of neighboring concavities intersect to form a network of nearly square cavities that preserve the array dimensions of each the intersecting layers (Figs 4D,E, 5H). In blue *T. urvillianus* and green *T. priamus,* the upper surfaces of the scales are covered with prominent, cone-shaped ridges, and the organization of the air cavities within the body of the scales is substantially less regular (Fig. 5A–C). In *Celastrina ladon,* two or three layers of rectangular air cavities comprise almost the entire body of the scale (Fig. 5D).

Previously classified as internal, diffraction arrays (Type IIIa of Vukusic et al., 2000a), *Parides sesostris* (Papilionidae), *Callophrys dumetorum* and *Mitoura gryneus* (Lycaenidae) are all characterized by a complex crystal-like array of spherical air cavities that are interconnected to one another in a tetrahedral nanostructure (Figs 4H–J, 5E–G). Two-dimensional sections through these nanostuctures reveal the extraordinary complexity of these air bubble arrays. In addition, the entire dorsal surface of the *Parides sesostris* scales is covered with a complex network of vertical ridges that create large elliptical air spaces (Fig. 4H). Although the

possible optical function of these superficial structures is unknown, the structural colour is produced by the arrays in the body of the scale (Ghiradella, 1985; Ghiradella, 1991; Vukusic and Sambles, 2003).

Papilio zalmoxis has been proposed to produce a blue colour by Tyndall scattering (Huxley, 1976; Type IIIb of Vukusic et al., 2000a). *Papilio zalmoxis* has a quite distinct structure of tubular channels approximately 200 nm in diameter that run nearly vertically from the dorsal surface of the scale to its basal lamina (Fig. 4F,G) (Huxley, 1976; Ghiradella, 1985; Ghiradella, 1998). However, the tubular channels are less than perfectly vertical as depicted by Huxley (1976), and may meander slightly horizontally (Fig. 4F).

Although only *Morpho aega* and *Troides brookiana* produced structural colours primarily with laminar superficial scale ridges, as previously recognized (Vukusic et al., 2001a) other species also showed some type of periodic ornamentation on the ridges of the scales, including *Urania fulgens* (Fig. 4A), *Papilio ulysses* (Fig. 4D), *Papilio zalmoxis* (Fig. 4F), *Troides urvillianus* (Fig. 5A) and *Troides priamus*.

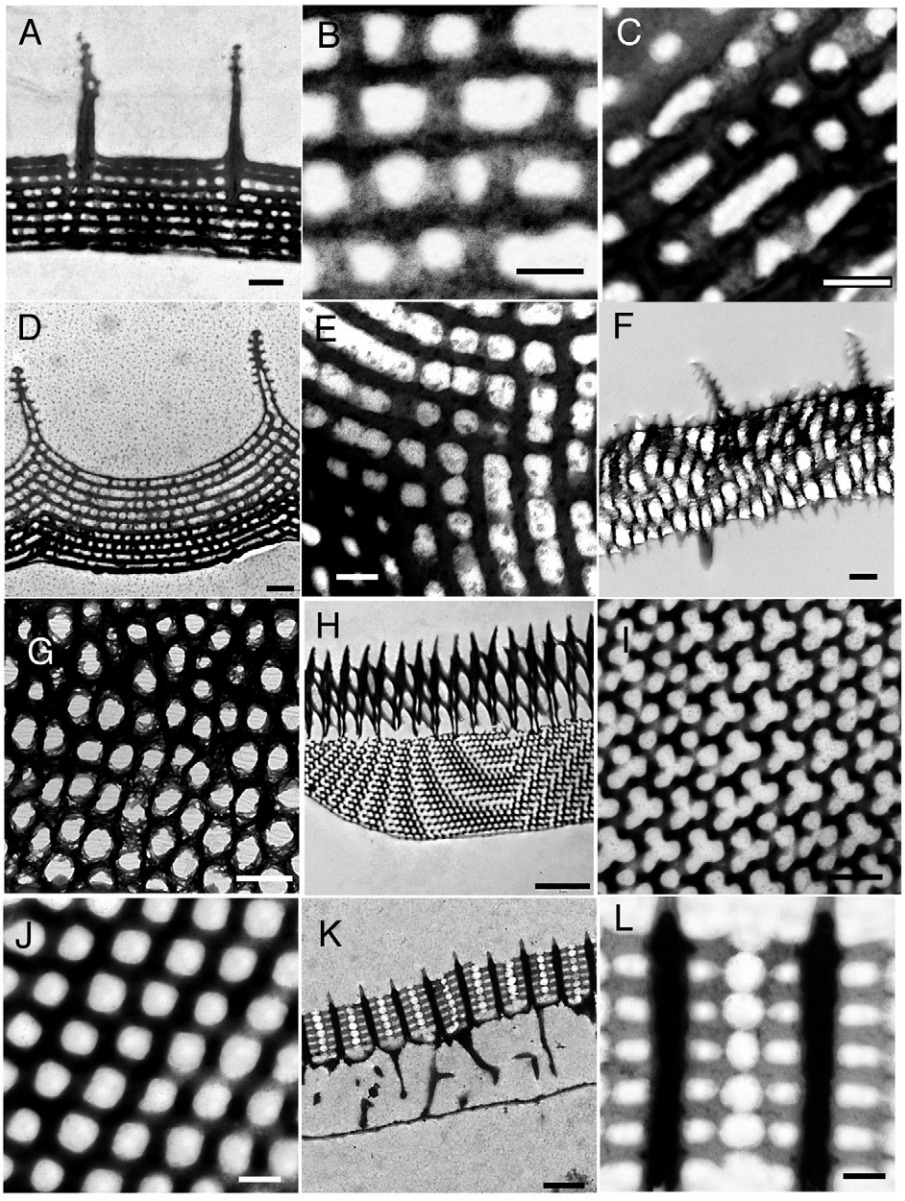

Fig. 4 Transmission electron micrographs (TEMs) of sections of the structurally coloured scales of a sample of the lepidopteran species examined. (A,B) *Urania fulgens* blue, (C) *Urania fulgens* green, (D,E) *Papilio ulysses,* (F,G) *Papilio zalmoxis*, (H–J) *Parides sesostris,* (K,L) *Troides brookiana*. Scale bars, 500 nm (A,D, F,G), 200 nm (B,C,E,J,L), 2 μm (H), and 1 μm (K).

Fourier power spectra

The 2D Fourier analyses of the colour producing arrays from butterfly scales reveal three general patterns of nanostructure (Fig. 6). Regardless of whether they are internal to the scale or formed by superficial scale ridges, laminar arrays showed two points of high Fourier power values above and below the origin, indicating that the predominant periodicity in these nanostructures consists of intermediate spatial frequencies in the vertical direction: e.g. *Urania fulgens* (Fig. 6A), *Troides urvillianus* (Fig. 6F), *Parrhasius moctezuma* (Fig. 6H) and *Morpho aega* (Fig. 6I; power spectrum is rotated 45° in orientation as were the arrays in the original TEM).

Deviations from this simple 1D distribution of Fourier power reveal additional details about variations in laminar nanostructure. The Fourier power spectra of the laminar ridge structures of *Troides urvillianus* showed the typical vertical pair of dots indicating highly laminar nanostructure, but it also had high Fourier power values at a broad range of smaller spatial frequencies in the horizontal plane (Fig. 6E). These lateral Fourier power peaks document the periodicity of the larger spacing between neighboring ridges along the surface of the scale (Fig. 4K,L).

In *Papilio ulysses*, Fourier power spectra of TEMs taken from the region of the scales immediately below the superficial ridges where the curved multilayers of air cavities from adjacent concavities in the scale intersect (Fig. 4E) reveal two prominent directions of equivalent nanostructure separated by ~45° (Fig. 6B). Similar results were observed in power spectra from similar TEMs from *Parrhasius moctezuma* (Fig. 5H). These power

spectra demonstrate that the laminar arrays within each scale concavity preserve a consistent nanostructure despite the distortions from a simple plane and their superimposition at the intersections of the concavities.

The less organized but generally laminar systems found in *Troides urvillianus* and *T. priamus hecuba* revealed a tendency toward a broader distribution of Fourier power in a ring of values in all directions of equivalent spatial frequency (e.g. Fig. 6F).

Crystal-like arrays of air cavities showed power spectra with hexagonal distribution of Fourier power values arranged in the directions of nearest neighbor cavities: e.g. *Parides sesostris* (Fig. 6D) and *Callophrys dumetorum* (Fig. 6G). These hexagonal power spectra show that periodicity is distributed along each of the lines of symmetry within the tetrahedral arrays.

TEM sections at different angles through the scales of *Papilio zalmoxis* showed an array of elliptical (Fig. 4F) or circular (4G) air spaces that were nearly vertical in orientation and which yielded either oval or circular distributions of Fourier power (Fig. 6C based on Fig. 4G). These results indicate that the tubular air cavities in *Papilio zalmoxis* are not spatially independent of one another over the spatial scale of visible light waves as assumed by the incoherent, Tyndall or Rayleigh scattering mechanisms.

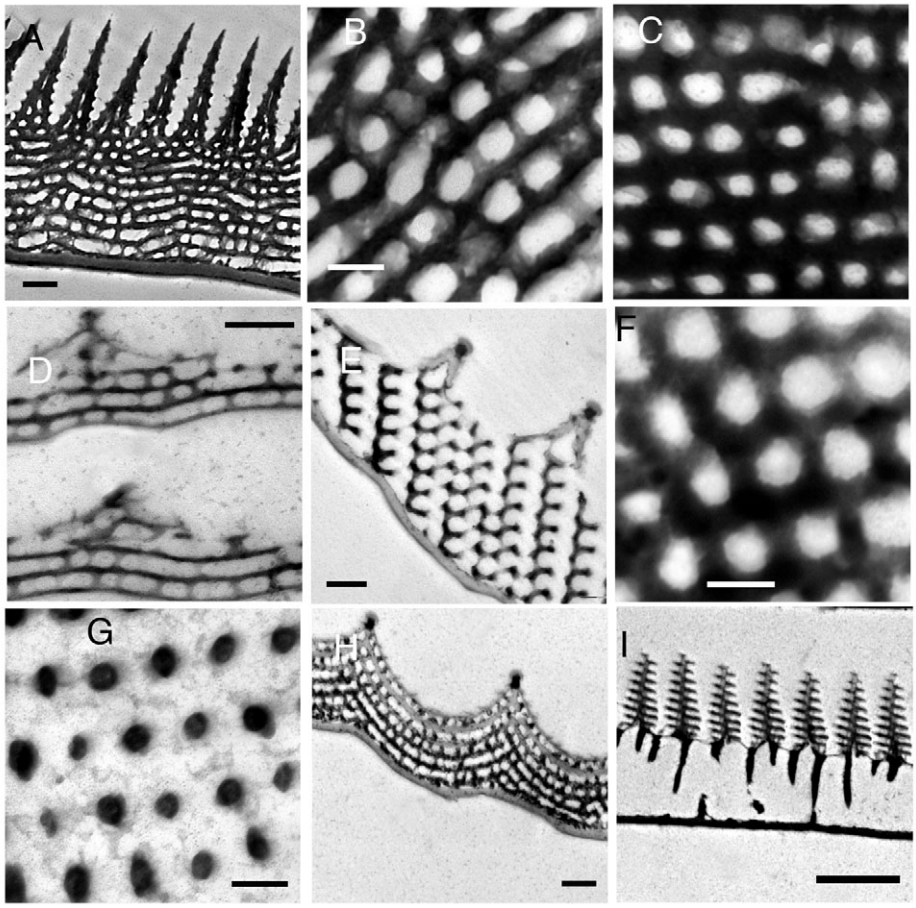

Fig. 5. Transmission electron micrographs (TEMs) of the structurally coloured scales of a sample of the Lepidoptera examined. (A-B) *Troides urvillianus*, (C) *Troides priamus*, (D) *Celastrina ladon*, (E,F) *Callophrys dumetorum*, (G) *Mitoura gryneus*, (H) *Parrhasius moctezuma*, (I) *Morpho aega.* Scale bars, 500 nm (A,D,E,H), 200 nm (B,C,F,G), and 2 μm (L).

Radial average of power spectra

Radial averages of the Fourier power spectra demonstrate that the peak spatial frequencies of variation in refractive index within the structurally coloured butterfly wing scales are within the range of values that would be expected to produce visible colours by coherent scattering (Fig. 7). Thus, the Fourier power spectra indicate that the colour producing arrays in the butterfly scales are appropriately nanostructured to produce a visible colour by coherent scattering.

Fourier predicted reflectance spectra

The predicted peaks of reflectance based on radial or sectional averages of the Fourier power spectra showed reasonable correspondences with the measured reflectance peaks in most of the 13 specimens analyzed (Figs 8, 9; Table 2). The most accurate predictions of peak hue (⩽20 nm of error) were for *Urania fulgens* blue (Fig. 8A), *Parides sesostris* (Fig. 8E), *Troides brookiana* (Fig. 8F), *Troides urvillianus* (Fig. 9B), *Celastrina ladon (*Fig. 9C), *Callophrys dumetorum* (Fig. 9D) and *Morpho aega* (Fig. 9G). These samples include external laminar (Type I), internal laminar (Type II) and internal crystal-like arrays (Type IIIa). More error (20–35 nm) existed in the predicted peak hue of *Urania fulgens* green (Fig. 8B), *Papilio ulysses* (Fig. 8C), *Troides priamus* (Fig. 9B), *Mitoura gryneus* (Fig. 9E) and *Parrhasius moctezuma* (Fig. 9F). Yet, in all cases, the predicted reflectance spectra showed prominent peak hues within the visible range, indicating that these colours are produced by coherent scattering.

In most instances, the 2D Fourier power spectra did not predict the detailed shape of the butterfly scale reflectance spectra (exceptions include Figs 8A,E, 9A). This could be due the limited samples of scales examined and micrographs taken in this broad survey. Also, the 2D Fourier power spectra from complex 3D organizations can gave a distorted view of the overall nanostructure. Images of sections through a plane of fusions among adjacent air cavities could indicate an increased size of the air cavities and result in exaggerating the size of the overall periodicity (e.g. Figs 4I, 5E).

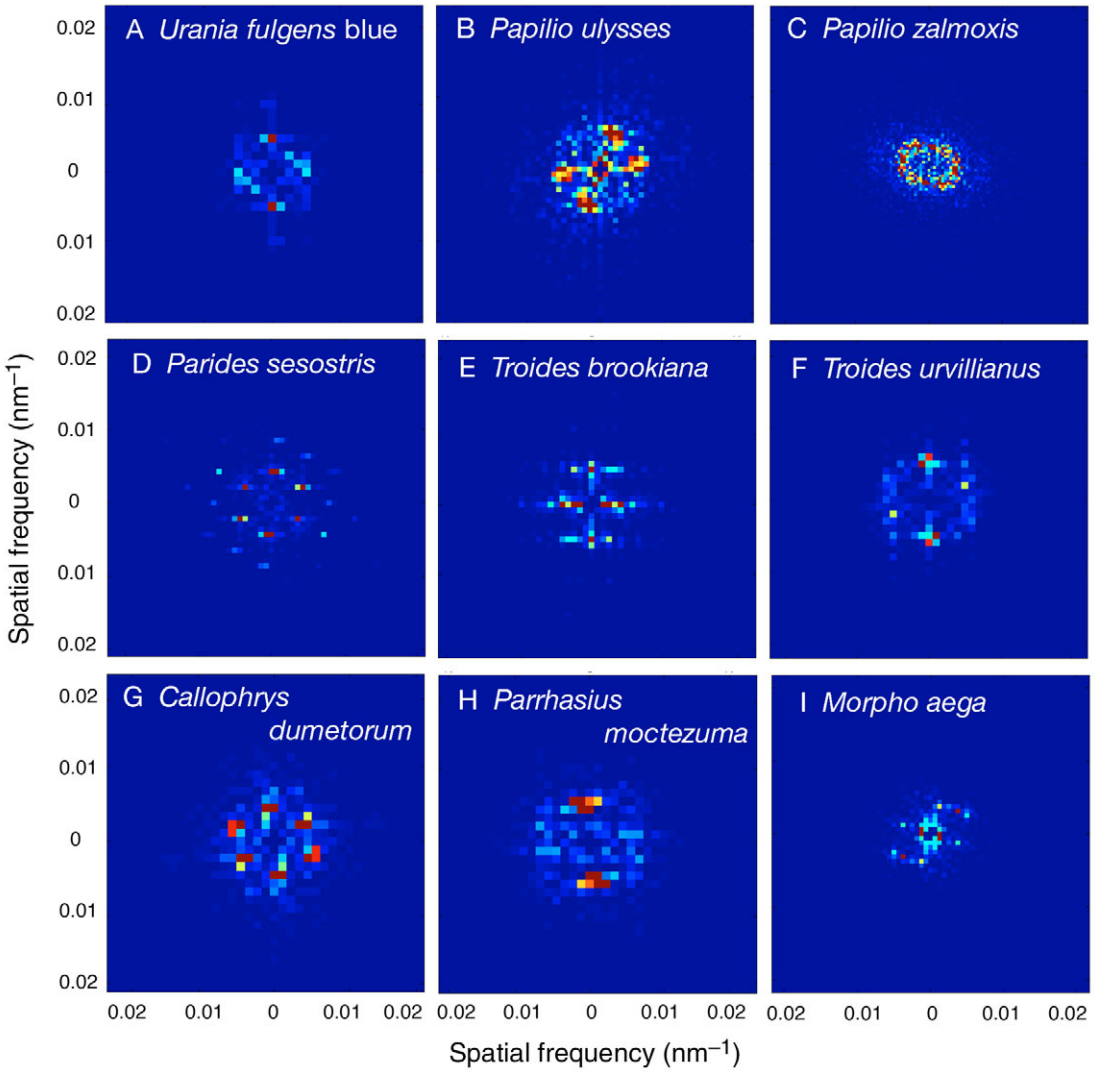

Fig. 6. Two-dimensional Fourier power spectra of transmission electron micrographs of structural colour producing butterfly scale nanostructures (Figs 4, 5). (A) *Urania fulgens* blue (Fig. 4B), (B) *Papilio ulysses* (Fig. 4E), (C) *Papilio zalmoxis* (Fig. 4G), (D) *Parides sesostris* (Fig. 4J), (E) *Troides brookiana* (Fig. 4L), (F) *Troides urvillianus*, (G) *Callophrys dumetorum* (Fig. 5F), (H) *Parrhasius moctezuma* (Fig. 5H) and (I) *Morpho aega* (not illustrated). Colour scale (from blue to red) indicates the relative magnitude of the squared Fourier components, which are dimensionless quantities. Direction from the origin indicates the direction of the 2D component waves in the image, and the distance from the origin indicates the spatial frequency (cycles/nm) of each Fourier component. The Fourier power peaks (red pixels) demonstrate predominant periodicities at intermediate spatial frequencies. The distance from the origin is inversely proportional to the wavelength of the coherently scattered colour.

The Fourier predicted reflectance spectrum for *Papilio zalmoxis* features a prominent peak at 740 nm, which would be expected for coherent scattering from a complex array of larger air cavities (~200 nm in diameter) (Fig. 8D). This peak is completely unrelated to the measured peak hue of 474 nm for directly incident light (Fig. 8D). However, it is congruent with the yellow luster that *P. zalmoxis* shows at a shallow angle of view (Huxley, 1976). At shallow angles, light waves should coherently scatter efficiently from the vertical air channels within the scales. The Fourier analysis of *P. zalmoxis* indicates that the shorter visible wavelengths of light that are scattered by neighboring air cavities will be non-randomly out of phase with each other, and will cancel out upon scattering. Therefore, the observed periodicity falsifies the underlying assumption of the hypothesis that incoherent Tyndall scattering contributes to the production of this blue colour (Huxley, 1976) (see Discussion).

Discussion

Two-dimensional Fourier analyses of the colour producing scales from a diversity of butterfly species confirm that these scales are appropriately nanostructured to produce visible colours by coherent scattering alone. Regardless of their anatomical position (on the surface or within the scale) or their spatial organization (multilayer or crystal-like), structural colour producing butterfly scale nanostructures share a common

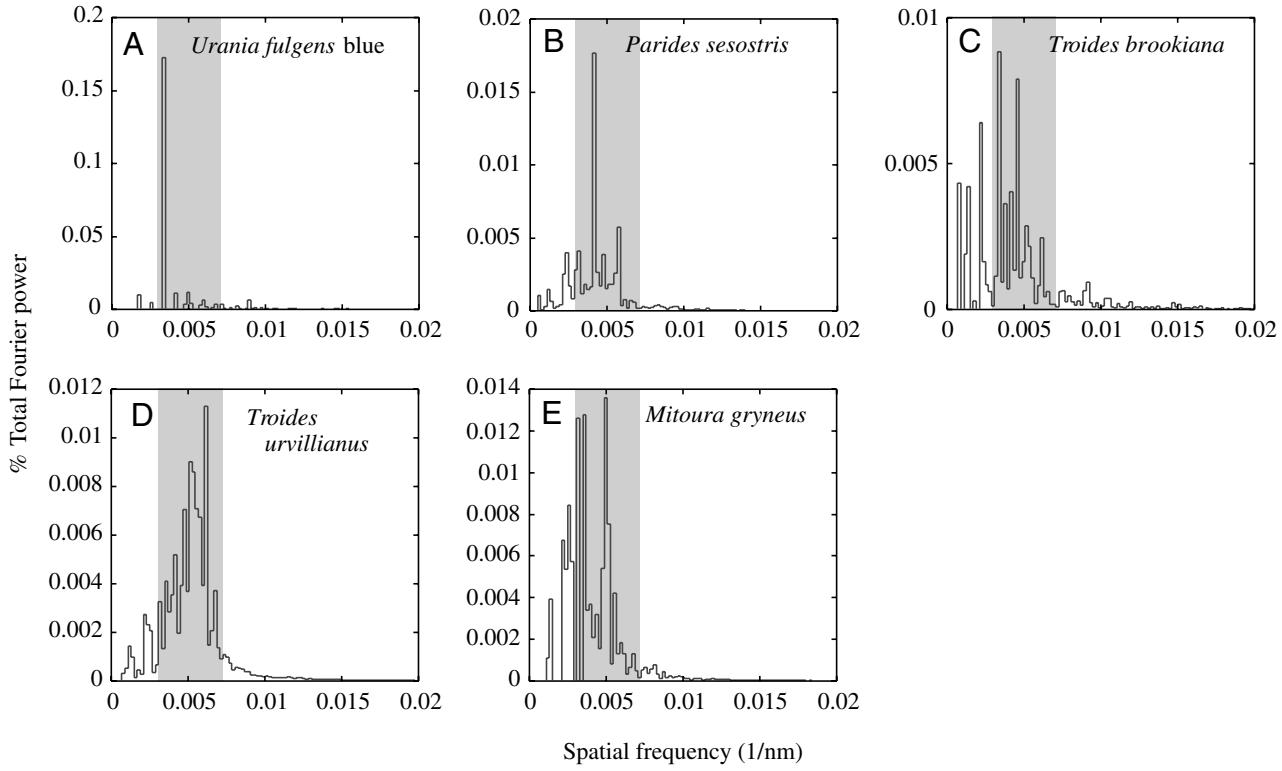

Fig. 7. Radial averages of two-dimensional Fourier power spectra from TEM micrographs of structural colour producing butterfly scale nanostructures (Fig. 6). (A) *Urania fulgens* blue, (B) *Parides sesostris*, (C) *Troides brookiana,* (D) *Troides urvillianus*, (E) *Mitoura gryneus.* The shaded zone shows the range of spatial frequencies that are likely to produce coherent scattering of visible light wavelengths.

physical mechanism of colour production: coherent scattering, i.e. the differential reinforcement and interference of visible wavelengths by light scattering from nanostructural spatial periodicities in refractive index. The singular exception to this conclusion, *Papilio zalmoxis*, is discussed in detail below.

The Fourier predicted reflectance peaks corresponded to within 15 nm of the measured reflectance peaks for the majority of species examined, including those with colour producing nanostructures from all previously recognized, major classes of nanostructure: multilayer external lamina, multilayer internal lamina, and internal crystal-like nanostructures (Types I, II and IIIa).

We examined blue and green scales from the same individual of *Urania fulgens* (Type I; Figs 1A, 2A–C, 4A–C, 8A,B), and blue and green scales from the two closely related species *Troides urvillianus* and *T. priamus* (Type II; Figs 1F,G, 2H,I, 5A–C, 9A,B). In both cases, the Fourier analyses correctly predicted the differences in hue between the conspecific samples. Interestingly, in both instances, the nanostructures producing the longer wavelengths are characterized by both smaller spatial frequencies of periodicity (i.e. larger lattice spacing), and smaller air cavity size (Figs 4B,C, 5B,C). Along with the increase in array dimensions, the reduction in cavity size will raise the volume fraction of chitin in the array, raising the average refractive index of the tissue, and further contributing to a longer wavelength coherent scattering. Additional comparative studies are required to determine if this pattern is generalizable to other lepidopterans.

While exploiting the common physical mechanism of coherent scattering, Lepidoptera have evolved extraordinary anatomical diversity and complexity in nanostructure. Many of these anatomical variations create additional optical effects beyond hue itself, including iridescence, highly or partially polarized reflections, and colour mixing effects (Ghiradella, 1985; Ghiradella, 1991; Vukusic et al., 1999; Vukusic et al., 2000a; Vukusic et al., 2000b; Vukusic et al., 2001a; Vukusic et al., 2001b; Vukusic et al., 2002).

Papilio zalmoxis

Papilio zalmoxis is the only lepidopteran that has been specifically hypothesized to produce structural colour by incoherent, Tyndall scattering (Huxley, 1976). Although Huxley's Tyndall scattering hypothesis for *P. zalmoxis* was not questioned in subsequent literature (e.g. Nijhout, 1991; Ghiradella, 1998; Parker, 1999; Vukusic et al., 2000a), Huxley actually expressed substantial uncertainty in his original paper. His complex final description of the blue colour in male *Papilio zalmoxis* was '*A basic Tyndall scattering spectrum... is modified by thin film action of the basement lamella and by strong pigmentary absorption in the violet and u.v.*' Further, he conceded that his proposed mechanism '*would be complicated by multiple scattering and by the partial irregularities of the alveolar arrays*'.

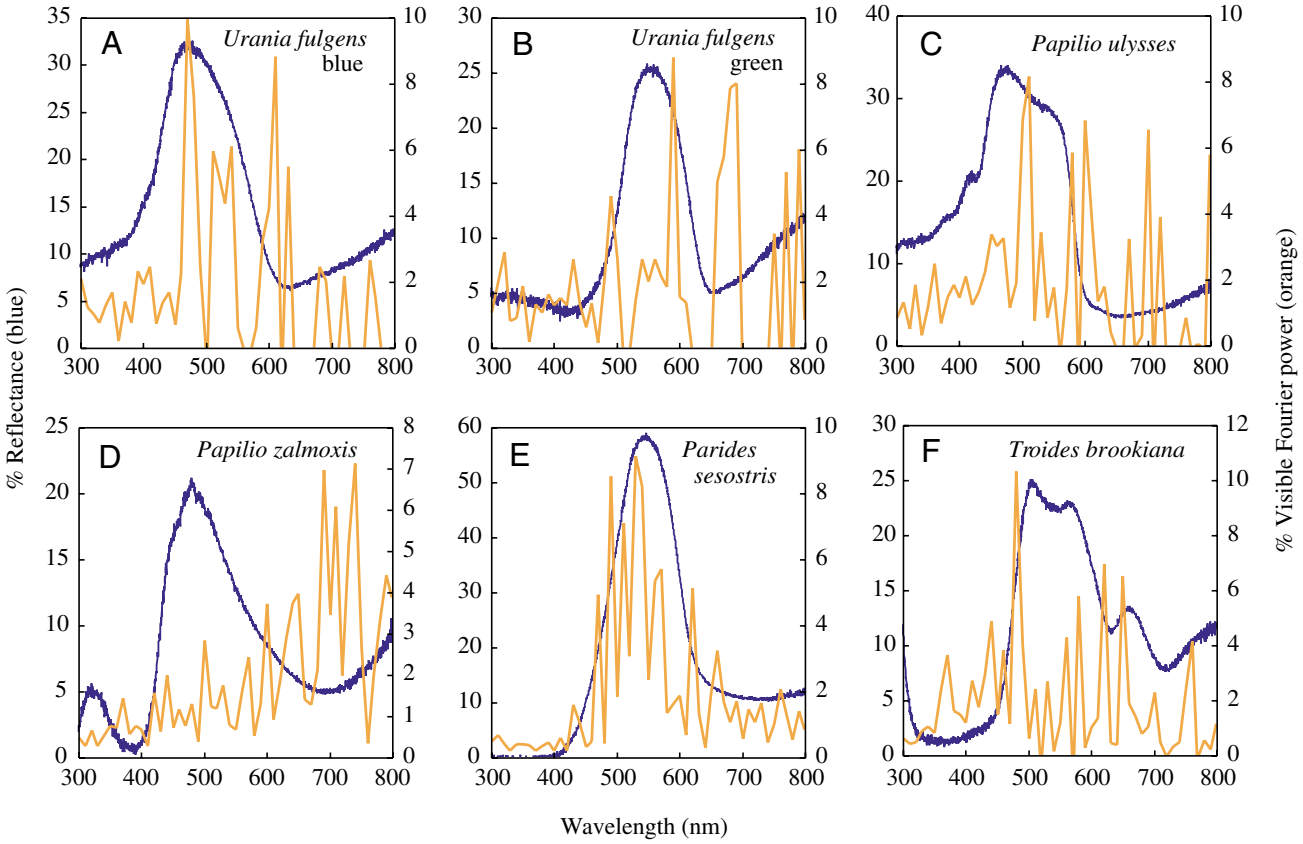

Fig. 8. Measured reflectance spectra (blue) and Fourier predicted reflectance spectra (orange) for the structurally coloured butterfly nanostructures illustrated in Fig. 4. (A) *Urania fulgens* blue, (B) *Urania fulgens* green, (C) *Papilio ulysses*, (D) *Papilio zalmoxis*, (E) *Parides sesostris*, (F) *Troides brookiana*.

The Fourier analyses conducted here provides the analysis of multiple scattering that was missing from Huxley's analysis (Huxley, 1976). Our results imply that the incoherent Tyndall component of Huxley's proposed mechanism does not occur. The vertical tubular cavities within scales are open at the top, and really inappropriate in shape for vertical light scattering. Light scattering can occur only from light incident on the sides or the bottom of these cavities, and not on the top surfaces. Therefore, the critical dimensions of the cavities are the neighbor-to-neighbor distances between cavities and not the vertical height of the tubes. TEM cross-sections of the scales produce a diversity of profiles of the tubular cavities from highly elliptical to perfectly circular, depending apparently on the angle of the cross sections and the variation in the orientation of the tubular cavities (Fig. 4F–G). The majority of light scattering must be produced by the sides of the tubes. The Fourier power spectra of these tubular spaces document a distinct and repeatable nanoperiodicity at a spatial scale appropriate for the coherent scattering of a longer wavelength visible colour (Figs 6C, 8D). This result can be easily understood given the large (>200 nm) diameter of the spaces and the additional distance between nearest neighbors (Fig. 4G). Light scattering from these tubular air cavities will be coherent scattering of longer visible wavelengths, not incoherent scattering of smaller visible wavelengths. Smaller visible wavelengths scattered by neighboring cavities will be predictably out of phase, resulting in destructive interference among these wavelengths. This result is inconsistent with the hypothesis of incoherent scattering by these nanostructures. Huxley remarked that *Papilio zalmoxis* produce a yellow luster when viewed at 'grazing angles' (Huxley, 1976). This easily observed yellow hue is clearly structural since it disappears with the application of a high refractive index fluid (e.g. isopropanol). Apparently, this yellow color is coherently scattered light from neighboring nanocavities.

Huxley's hypothesis was weakly supported by his own data (Huxley, 1976). The reflectance spectra of *Papilio zalmoxis* after extraction of a fluorescent pigment (provisionally identified as a kynurenine) shows only the slightest of increases in scattering of short wavelengths and also increases at longer wavelengths above 550 nm (fig. 10 in Huxley, 1976). The reflectance spectrum of the pigment extracted scales does not conform at all to the Rayleigh scattering prediction that the magnitude of scattering will be inversely proportional to the fourth power of the wavelength (van de Hulst, 1981; Young, 1982; Bohren and Huffman, 1983), as Huxley (1976) proposed. Rather, the resulting reflectance spectra had entirely lost the blue hue and are essentially colorless (fig. 10 in Huxley, 1976). Furthermore, the emission spectrum of the fluorescent pigment matches the reflectance spectrum of the

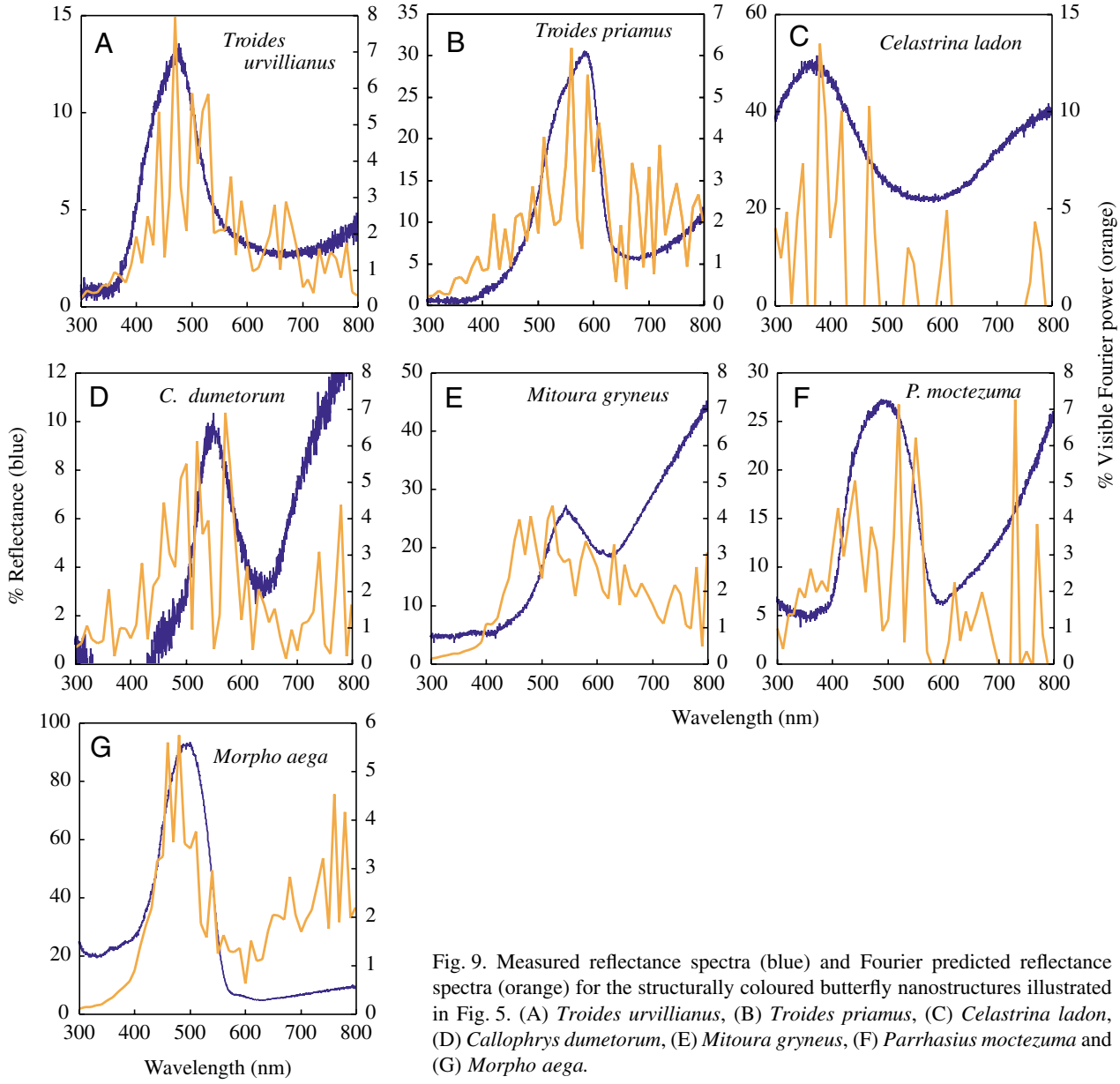

Fig. 9. Measured reflectance spectra (blue) and Fourier predicted reflectance spectra (orange) for the structurally coloured butterfly nanostructures illustrated in Fig. 5. (A) *Troides urvillianus*, (B) *Troides priamus*, (C) *Celastrina ladon*, (D) *Callophrys dumetorum*, (E) *Mitoura gryneus*, (F) *Parrhasius moctezuma* and (G) *Morpho aega.*

scales almost exactly (fig. 12 in Huxley, 1976). Thus, Huxley's data strongly support the conclusion that the blue of *Papilio zalmoxis* is essentially a pigmentary colour.

In conclusion, the hypothesis of incoherent Tyndall scattering by *Papilio zalmoxis* is not supported by our Fourier analyses or by Huxley's own data. The blue colour of *Papilio zalmoxis* is produced by a fluorescent pigment. Apparently, the function of the tubular nanostructure within the scale is to provide internal surfaces for the deposition of the pigment (Huxley, 1976), and to coherently scatter incident light horizontally into the fluorescent pigment molecules on adjacent alveolar surfaces and increase the brilliance of the pigment. Interestingly, in addition to coherently scattering a long wavelength visible color at the ~740 nm, the tubular nanostructure of *P. zalxmoxis* should also coherently scatter wavelengths that are one half this size, or approximately 370 nm. This wavelength is very close to the excitation maximum of the kyurenine pigment extracted from *P. zalmoxis* (Huxley, 1976)

Recently, Vukusic and Hooper (2005) came to a similar conclusion for a closely related species, *Papilio nireus*, which has apparently identical anatomy and nanostructure. Vukusic and Hooper concluded also that this nanostructure is designed to coherently scatter light wavelengths in the horizontal plane to increase the flourescence of the blue pigment. Based on a photonic analysis of an idealized crystal-like array, they propose that the nanostructure is tuned to coherently scatter wavelengths that are near to the observed reflectance peak. However, our analysis implies that this nanostructure should produce a peak reflectance at much longer visible wavelengths. The predominant spatial frequency we had documented (Fig. 6C) is replicated exactly in Fourier analysis presented in

the supplementary materials by Vukusic and Hooper (fig. S4 in Vukusic and Hooper, 2005). Our prediction is also congruent with the yellow luster observed at shallow angles in both *P. zalmoxis* and *P. nireus*, which is clearly a structural color (see above). So far, the analysis of Vukusic and Hooper (2005) provides no explanation of the origin of this yellow structural color. Further research may be necessary to establish the source of this disparity.

In previous papers, we have tested and rejected the traditional hypothesis of incoherent Rayleigh scattering for noniridescent structural colours in avian feather barbs (Prum et al., 1998; Prum et al., 1999b; Prum et al., 2003), avian skin (Prum et al., 1999a; Prum et al., 2003b), mammalian skin (Prum and Torres, 2004), odonate integument (Prum et al., 2004), and now butterflies. We know of no examples of incoherent scattering in organisms that have been supported by both reflectance spectra showing congruence with Rayleigh's inverse fourth power law, and with evidence that the light scatterers are spatial independent. Thus, all proposed examples of organismal incoherent scattering require further testing.

Iridescence

Fourier analyses of scale nanostructures provide insights into how iridescence – strong directionality in color – can be created or suppressed by variation in nanostructure. Laminar arrays from butterfly scales displayed single Fourier power peaks at intermediate spatial frequencies above and below the origin (Fig. 6); these peaks document that periodicity in array nanostructure is not equivalent in all directions. This condition will produce strong directionality in back scattering, resulting in iridescence, or prominent changes in hue with angle of observation and illumination (Prum and Torres, 2003a). Interestingly, Wickam et al. (2005) have recently documented that laminar nanostructures from the ridge lamellae and tilted microribs are more highly iridescent than are scales with horizontal microribs.

Hexagonal, crystal-like arrays of air bubbles also provide some nanostructural opportunities for iridescence, but this iridescence is often reduced by variation at larger spatial scales in the orientation of the array among multiple cells of the butterfly scale (e.g. Figs 4H, 5E). The underlying opportunities for iridescence in these butterfly scales can still be observed in the occasional, sparkling, opalescent highlights of red and gold produced by the crystal-like nanostructures of green *Callophrys dumetorum* and *Mitoura gryneus* scales (Fig. 3B,C). The dense and complex ridges on the scales of *Parides sesostris* (Fig. 4H) may be to diffuse the structural colour produced by the underlying nanostructure uniformly over many directions.

The scales of some laminar butterfly nanostructures reduce iridescence by having concavities in the scale surface that distort the planar orientation of their multilayer nanostructures (e.g. *Papilio ulysses*, and *Parrhasius moctezuma*; Figs 4D, 5J). A 2D Fourier analysis of a single scale concavity from *Papilio ulysses* shows an arc of high power spectrum values at a broad range of angles for a single prominent spatial frequency (Fig. 10). This arc-shaped power spectrum indicates that the concavity expands the directions over which the scale nanoperiodicity is equivalent, and creates a wider range of directions over which directly backscattered light will coherently scatter the same peak hue. The result is a uniformity of colour with angle of observation under general omnidirectional, natural lighting, and a reduction in the iridescence produced by a laminar nanostructure. The scale concavities of *Papilio ulysses* and *Parrhasius moctezuma* are functionally analogous and strikingly similar to the iridescence reducing convexities of the laminar arrays of melanin granules in feather barbules of some fruit pigeons (Dyck, 1987) and cuckoos (Durrer and Villiger, 1970), which show similar arc-shaped power spectra (Prum, 2006).

Likewise, the deviations from a uniformly laminar orientation in the nanostructure of *T. priamus* across multiple ridges is also likely to function in expanding the angles over which the primary hue is observed (Fig. 5A). This relaxed laminar organization approaches the non-iridescent, quasiordered nanostructures at larger spatial scales (Prum et al., 1998; Prum et al., 1999a; Prum et al., 1999b; Prum and Torres, 2003a; Prum and Torres, 2003b; Prum and Torres, 2004).

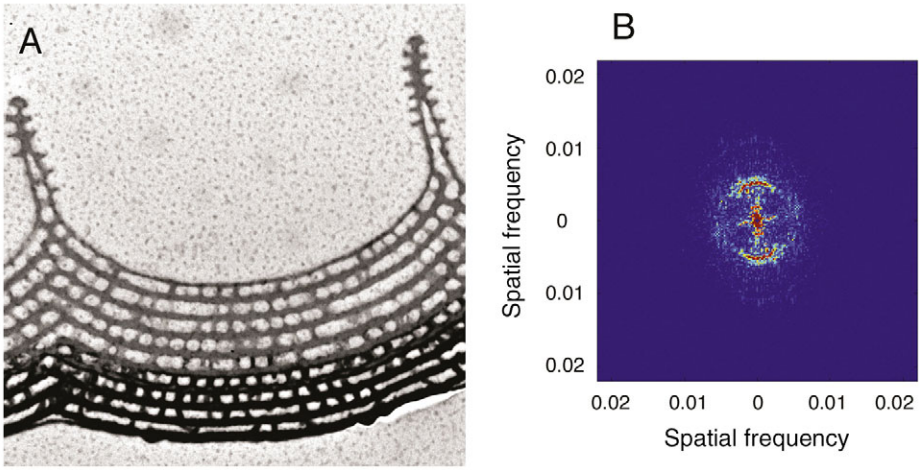

Fig. 10. Fourier analysis of a concavity from a structurally coloured scale of *Papilio ulysses*. (A) Transmission electron micrograph of a single scale surface concavity from *Papilio ulysses*. (B) 2D Fourier power spectrum of A showing an arc-shaped distribution of Fourier power peaks (red pixels) above and below the origin that is created by the concave distortion of the fundamentally laminar array of air bubbles in the scale. The result is a broadening of the range angles over which the light back-scattered to the observer will maintain the same peak hue.

Butterflies with laminar arrays can also reduce iridescence by morphological adjustments at larger spatial scales. For example *Urania fulgens, Papilio ulysses*, *Troides urvillianus, T. priamus* and *Parrhasius moctezuma* all have prominently curved scales, which will contribute to the same optical effect (Figs 2A–E,H,I, 3D). The effects of these multiple methods of reducing iridescence can easily be observed by comparing the laminar but weakly iridescent *Papilio ulysses*, *Urania fulgens*, *Troides urvillianus*, *T. priamus* and *Parrhasius moctezuma* to the highly iridescent *Morpho aega*, which maintains both planar, laminar nanostructures and perfectly flat scales (Fig. 3F). These structural variations further underscore how anatomical variation can contribute to variation in optical function within a common physical mechanism.

Physics and evolution of butterfly structural colours

Although the mechanisms of structural colour production of butterflies and other organisms have been traditionally viewed as mechanistically diverse, this apparent diversity of optical phenomena is more productively understood as derived variations of coherent scattering, rather than as distinct phenomena based on different optical mechanisms. Although physically sophisticated readers may find this mechanistic unification to be trivial, ascribing different traditional optical categories to diverse biological anatomies has created substantial intellectual costs in the study of the evolution of biological nanostructure and optical function. For example, it has never been previously recognized that the common coherent scattering mechanism supports the likelihood that butterfly nanostructures have evolved among anatomical/optical classes while consistently retaining a structural color production function. As in avian feathers and skin (Prum et al., 1999b; Prum and Torres, 2003a; Prum, 2006), it appears that many butterfly clades have probably diversified evolutionarily among different anatomical classes that have been previously classified as mechanistically distinct, and have traditionally required different, incompatible mathematical tools to analyze their optical function. Traditional optical analyses of these diverse structures would require distinct mathematical methods even if the ancestral forms had consistently maintained a coherently scattering optical function throughout their evolutionary history. Thus, following traditional methods, it would be impossible to analyze an evolutionary transition between a crystal-like array and a multilayer thin film, or a diffraction grating and a Bragg scatterer.

Traditional classifications of butterfly scale nanostructures may have created conceptual obstacles to understanding the evolution of nanoscale diversity. In contrast, understanding the common physical mechanism behind the morphological diversity provides insights into how the startling variety of nanostructures and optical functions could have evolved into one another as elaborations of a common physical mechanism.

A physicist may conveniently adopt the most appropriate tool for a given physical situation, but a biologist interested in the evolution of nanostructure and optical function must adopt an analytical tool that can span the multiple classes of nanostructural organization of the evolutionary histories of the organisms. Organismal evolution presents unique demands that have not been addressed by traditional optical techniques. In short, evolutionary biology may demand new physical approaches and methods.

These results provide an important insight into how diversity in nanostructure and optical function may have evolved in lepidopterans through selection on novelties in optical function. For example, the Fourier power spectra (Fig. 6B) of the intersections of the concave multilayers of air bubbles in *Papilio ulysses* (Fig. 4E) demonstrate how internal laminar (Type II) and internal crystal-like (Type IIIa) nanostructures can intergrade into one another. These scale concavities function and have likely evolved by selection to reduce iridescence (see above, Fig. 10), and have produced the periodic establishment across the scale of an intermediate form of nanostructure between laminar and crystal-like arrays (Figs 4E, 6B). It is easy to imagine how selection on optical function could lead to an evolutionary transition between these two types of nanostructures. Furthermore, the deeper concavities of *Papilio palinurus* that produce optical colour-mixing of yellow and blue (Vukusic et al., 2000b; Vukusic et al., 2001a) likely evolved as derived elaborations of the type of iridescence reducing concavities found in *Papilio ulysses*.

As previously recognized (Vukusic et al., 2001a), many of the species with colour producing, laminar nanostructures within the body of the scales also have superficial ridges with periodic ornamentation that quite likely also function in coherent scattering, e.g. *Urania fulgens* (Fig. 4A), *Papilio ulysses* (Fig. 4D), *Papilio zalmoxis* (Fig. 4F) and *Troides urvillianus* (Fig. 5A). These anatomical intermediates between traditional Type I and Type II scales indicate how these two classes of nanostructure are functionally continuous. Furthermore, vivid structural colours are ubiquitous in the genus *Troides* (Papilionidae). It is very likely that the extraordinarily different nanostructures of *Troides brookiana, T. urvillianus* and *T. priamus* have evolved from a structurally coloured common ancestor through persistent selection on optical function. Thus, recognizing that ridge lamellae (Type I) and interior air cavities (Type II and IIIa) both function by the same coherent scattering mechanism makes it easier to conceptualize the evolution of nanostructural diversity exhibited by butterfly clades.

Even within the small sample of species analyzed, there is evidence of extraordinarily detailed, convergent evolution in butterfly scale optical nanostructures among the four distantly related lepidopteran clades. The crystal-like arrays of air spheres in the scales of the papilionid *Parides sesostris* (Fig. 4H–J) are strikingly similar to those in the lycaenids *Callophrys dumetorum* and *Mitoura gryneus* (Fig. 5E–G). Further, the laminar arrays with iridescence reducing concavities of the papilionid *Papilio ulysses* (Fig. 4D,E) are extremely similar to those of the lycaenid *Parrhasius moctezuma* (Fig. 5H). Natural and sexual selection on the

optical properties of structurally coloured butterfly scales has produced identical anatomical solutions in phylogenetically independent lineages.

Future analyses of structural colour evolution in butterflies should investigate optical function of wing scales in a phylogenetic context, to document the patterns of origin, maintanence, diversification and convergence. Prum et al. (2004) have begun these analyses in odonates. Recently, Wickham et al. (2005) presented a phylogenetic analysis of the evolution of structurally colored butterfly scales with surface multi-layers (Type I). Unfortunately, the small, biased sample that they analyzed included too little taxonomic or structural diversity to be meaningful. The color-producing multilayer nanostructures found in various species of nymphalids and papilionids are not homologous, but the limited sample of species analyzed by Wickham et al. (2005) ensures that they will be. (Imagine a phylogenetic study of the evolution of red hair in mammals that analyzed only species with red hair.) Their exclusive focus on the evolution of superficial multilayer scales, to the exclusion of other classes of color producing nanostructures that are found in close relatives of the species sampled (e.g. within *Troides*), further documents the conceptual limitations created by traditional categories of optical mechanism.

Ghiradella (Ghiradella, 1974; Ghiradella and Radigan, 1976; Ghiradella and Radigan, 1985; Ghiradella and Radigan, 1989; Ghiradella and Radigan, 1991; Ghiradella and Radigan, 1998) has pioneered studies of the development of the colour producing nanostructures in butterfly scales. These fascinating investigations document that intricate optical nanostructures structures develop in a variety of different mechanisms, even within a single family (Ghiradella, 1989; Ghiradella, 1998). Functional, developmental and phylogenetic studies of a diversity of structurally coloured butterfly species within a major clade (e.g. Lycaenidae, Papilionidae, Nymphalidae) would provide exciting new data on the dynamics of structural colour evolution in lepidopterans. Previous research has provided advanced mathematical models (Nijhout, 1991) and detailed molecular mechanisms of wing pattern determination in butterflies (Carrol et al., 1994; Brunetti et al., 2001). Recent work has also examined the developmental correlation between scale structure and pigmentation (Janssen et al., 2001; Otaki and Yamamoto, 2004). None of this research has yet focused on the development of structural colouration patterning with its combination of extreme anatomical modifications of scales and complex distribution on the wing surfaces. For example, *Urania fulgens* shows variation in both wing pattern and structural colour that could be a new model species for this research program. Another premier experimental system for investigation of these processes could be *Precis octavia* (Nymphalidae) with an exceptional environmentally induced polyphenism in which homologous scales vary between structural blue or pigmentary orange or black (Nijhout, 1991).

Structural white

After focusing on the physics of production of wavelength specific structural colors in butterflies, it is appropriate to comment that broad spectrum white reflectance is also a common and important optical property of the scales of many butterflies. White is produced by incoherent scattering from unpigmented chitin of butterfly scales. The magnitude of scattering can be enhanced by the specific derived structures within various parts of the scale (e.g. Stavenga et al., 2004).

Polarized signals

We did not analyze polarization of the colors of these butterflies. Recently, Sweeney et al. (2003) have shown that polarized structural colors function in intersexual communication in *Heliconius cydno*. Although only structural colors can be polarized, not all structural colors are polarized. Many coherently scattering nanostructures will not produce polarized reflections. In brief, polarized colors are produced by materials with periodic variation in refractive index in one or two dimensions. In butterflies, this corresponds to species that have ornamented outer ribs of the scales (Type I). However, not all nanostructures will produce polarized reflections. In particular, nanostructures with periodic 3D variation in refractive index are unlikely to produce strongly and predicatably polarized signals.

Uses and limits of the Fourier method

In a series of papers, we have developed a method using 2D Fourier analyses to study the physical mechanisms of structural colour production in organisms (Prum and Torres, 2003a). Originally, the method was developed to analyze colour production by quasiordered arrays of light scattering objects that could not be analyzed using traditional thin-film optics or Bragg scattering methods (Prum et al., 1998; Prum et al., 1999a; Prum et al., 1999b). We subsequently demonstrated that the method works effectively in describing coherent scattering by crystal-like and laminar nanostructures (Prum and Torres, 2003b; Prum and Torres, 2003a).

The use of the Fourier transform in this context can be justified on first principles. Electromagnetic radiation scattering from any periodic crystal will produce the reciprocal lattice of the crystal that is equivalent to its Fourier transform. The inverse Fourier transform of the reciprocal lattice will reconstruct the crystal lattice. Thus, essentially identical methods are used in crystallography to understand x-ray diffraction, an analogous process at a different spatial scale. Furthermore, like the Fourier method (Prum and Torres, 2003a), modern photonic methods proceed by characterizing the periodic variations in optical potential of a dialectric medium in order to describe its optical properties (Joannopoulos et al., 1995). Thus, the Fourier method fits squarely within the current direction of optical research.

An advantage of the 2D Fourier method is that it applies directly to TEMs – the original data on nanostructure – rather than to idealized measurements of the biological structures. These analyses are based on the real biological variations in nanostructure that are typically ignored in traditional optical analyses. Along with this advantage come the disadvantages caused by distortions to the nanostructure during observation

and the biases introduced by finite samples of images of complex nanostructures (Prum et al., 1999a; Prum and Torres, 2003a; Prum and Torres, 2003b; Prum and Torres, 2004).

Many methods of optical analysis of biological nanostructures are available. Thin-film optical methods (Macleod, 1986) have been applied with great success to laminar arrays in butterfly scales (e.g. Vukusic et al., 1999; Vukusic et al., 2000b; Vukusic et al., 2001a; Vukusic et al., 2001b; Vukusic et al., 2002). More recently, highly detailed optical diffraction models have been applied to complex 3D surface nanostructures in *Cynandra* (Nymphalidae) (Brink and Lee, 1999). For crystal-like nanostructures, Morris (1975) and Allyn and Downey (1976) provided only very general, approximate analyses of 3D diffraction in *Callophrys rubi* and *C. siva* (Lycaenidae). The 2D Fourier method is not going to replace advanced thin film and diffraction methods that can surpass it in accuracy in appropriate contexts. However, the Fourier method has advantages of being practical, easily calculated, and applicable to a diversity of nanostructures (Prum and Torres, 2003a). Other previous methods assume the nanostructure and its periodicity, but the Fourier method can establish the existence of the nanostructure itself. The Fourier method is the only current method applicable to quasi-ordered nanostructures, which lack explicit laminar or crystal-like periodicity. Further, the 2D Fourier method substantially improves upon the previous Bragg methods that have been applied to crystal-like arrays of butterfly scales (e.g. Morris, 1975; Allyn and Downey, 1976). The biggest advantage of the Fourier method is to provide insights into evolutionary transitions in nanostructural organization that are beyond the abilities of other, inflexible and incompatible methods of analysis. Indeed, the fact that researchers have not previously recognized the potential for evolution among different structural classes of coherently scattering butterfly nanostructures (Types I–IIIa) documents the intellectual cost of exclusively employing highly accurate physical methods with little generality.

Predicting the reflectance spectrum from the Fourier power spectrum requires a transformation from units of spatial frequency to wavelength. As we have realized and Soffer and Lynch (1999) have observed, the position of the reflectance peak will shift, depending upon whether it is expressed in frequency or wavelength units. In earlier applications of the method, we expressed predicted reflectance spectra using uniform frequency bins (Prum et al., 1998; Prum et al., 1999a; Prum et al., 1999b), whereas in more recent applications, we have used uniform wavelength bins (Prum et al., 2003; Prum and Torres, 2003a; Prum and Torres, 2003b; Prum et al., 2004; Prum and Torres, 2004). Both are correct, but there is some inherent variation in the predictions of the two methods. (A related issue occurs with establishing *a priori* the size and number of the bins themselves.) However, as Soffer and Lynch (1999) also observe, the magnitude of the shift in the position of the peak will depend on its breadth. Given that color producing biological nanostructures are so highly ordered (e.g. Fig. 6), there is a relatively small shift in the position of the peak. Experimentally, it is on the order of 15 nm or less. There is no absolutely preferred method to express this conversion. However (*contra* Soffer and Lynch, 1999), it is absolutely appropriate in this context to convert spatial frequency into wavelength because that is precisely what coherent scattering does. Variations in reflected wavelengths are produced by the interaction of ambient light waves with variation in refractive index over different spatial frequencies in the nanostructure. While inappropriate in some settings (Soffer and Lynch, 1999), transformation of spatial frequency into wavelength is the very essense of coherent scattering and structural color production.

A substantial challenge to the application of the Fourier method is presented by complex 3D nanostructures. Ultimately, it will be very productive to conduct 3D Fourier analyses of 3D data sets from high voltage electron microscopy or other tomographic techniques (e.g. Argyros et al., 2002).

We thank the J. S. Ashe of the Snow Entomology Collection of the University of Kansas Museum of Natural History for permitting the destructive sampling of lepidopteran specimens from the collection for this study. We thank Ray Pupedis of the Yale Peabody Museum of Natural History for the loan of specimens for photography (Fig. 1). Doekele Stavenga provided stimulating comments on the manuscript. The text was also improved by comments from three anonymous reviewers. Funds for the research were provided by grants from the National Science Foundation to the authors (DBI-0078376, DMS-0070514), and to the University of Kansas Department of Mathematics (DMS-0112375).

References

Allyn, A. C. and Downey, J. C. (1976). Diffraction structures in the wing scales of *Callophrys (Mitoura) siva siva* (Lycaenidae). *Bull. Allyn Mus.* **40**, 1-6.

Argyros, A., Large, M. C. J., McKenzie, D. R., Cox, G. C. and Dwarte, D. M. (2002). Electron tomography and computer visualization of a three-dimensional 'photonic' crystal in a butterfly wing-scale. *Micron* **33**, 483-487.

Benedek, G. B. (1971). Theory of transparency of the eye. *Appl. Opt.* **10**, 459-473.

Bohren, C. F. and Huffman, D. R. (1983). *Absorption and Scattering of Light by Small Particles.* New York: John Wiley and Sons.

Briggs, W. L. and Henson, V. E. (1995). *The DFT.* Philadelphia: Society for Industrial and Applied Mathematics.

Brink, D. J. and Lee, M. E. (1999). Confined blue iridescence by a diffracting microstructure: an investigation of the *Cynandra opis* butterfly. *Appl. Opt.* **38**, 5282-5289.

Brunetti, C. R., Selegue, J. E., Monteiro, A., French, V., Brakefield, P. M. and Carroll, S. B. (2001). The generation and diversification of butterfly eyespot color patterns. *Curr. Biol.* **11**, 1578-1585.

Carrol, S. B., Gates, J., Keys, D. N., Paddock, S. W., Panganiban, G. E. F., Selegue, J. E. and Williams, J. A. (1994). Pattern formation and eyespot determination in butterfly wings. *Nature* **265**, 109-114.

Downey, J. C. and Allyn, A. C. (1975). Wing-scale morphology and nomenclature. *Bull. Allyn Mus.* **31**, 1-32.

Durrer, H. and Villiger, W. (1970). Shillerradien des Goldkuckucks (*Chrysococcyx cupreus* (Shaw)) im Elektronenmikroskop. *Z. Zellforsch.* **109**, 407-413.

Dyck, J. (1987). Structure and light reflection of green feathers of fruit doves (*Ptilinopus* spp.) and an imperial pigeon (*Ducula concinna*). *Biol. Skrifter (Copenhagen)* **30**, 2-43.

Fox, D. L. (1976). *Animal Biochromes and Structural Colors.* Berkeley: University of California Press.
Ghiradella, H. (1974). Development of ultraviolet-reflecting butterfly scales: How to make an interference filter. *J. Morphol.* **142**, 395-410.
Ghiradella, H. (1985). Structure and development of iridescent lepidopteran scales: the Papilionidae as a showcase family. *Ann. Entomol. Soc. Am.* **78**, 252-264.
Ghiradella, H. (1989). Structure and development of iridescent butterfly scales: Lattices and laminae. *J. Morphol.* **202**, 69-88.
Ghiradella, H. (1991). Light and colour on the wing: structural colours in butterflies and moths. *Appl. Opt.* **30**, 3492-3500.
Ghiradella, H. (1998). Hairs, bristles, and scales. In *Microscopic Anatomy of Insects*, vol. 11A (ed. M. Locke), pp. 637-645. New York: Wiley-Liss.
Ghiradella, H. and Radigan, W. (1976). Development of butterfly scales. II. Struts, lattices and surface tension. *J. Morphol.* **150**, 279-298.
Hecht, E. (1987). *Optics.* Reading: Addison-Wesley Publishing.
Herring, P. J. (1994). Reflective systems in aquatic animals. *Comp. Biochem. Physiol.* **109A**, 513-546.
Huxley, A. F. (1968). A theoretical treatment of the reflexion of light by multi-layer structures. *J. Exp. Biol.* **48**, 227-245.
Huxley, J. (1975). The basis of structural colour variation in two species of *Papilio*. *J. Entomol. A* **50**, 9-22.
Huxley, J. (1976). The coloration of *Papilio zalmoxis* and *P. antimachus*, and the discovery of Tyndall blue in butterflies. *Proc. R. Soc. Lond. B* **193**, 441-453.
Janssen, J. M., Monteiro, A. and Brakefield, P. M. (2001). Correlations between scale structure and pigmentation in butterfly wings. *Evol. Dev.* **3**, 415-423.
Joannopoulos, J. D., Meade, R. D. and Winn, J. N. (1995). *Photonic Crystals: Molding the Flow of Light.* Princeton: Princeton University Press.
Kinoshita, S., Yoshioka, S. and Kawagoe, K. (2002). Mechanisms of structural colour in the *Morpho* butterfly: cooperation of regularity and irregularity in an iridescent scale. *Proc. R. Soc. Lond. B* **269**, 1417-1421.
Land, M. F. (1972). The physics and biology of animal reflectors. *Prog. Biophys. Mol. Biol.* **24**, 77-106.
Lee, D. W. (1997). Iridescent blue plants. *Am. Sci.* **85**, 56-63.
Macleod, H. A. (1986). *Thin-film Optical Filters.* Bristol: Adam Hilger, Ltd.
Mason, C. W. (1923). Structural colors of feathers. I. *J. Phys. Chem.* **27**, 201-251.
Morris, R. B. (1975). Iridescence from diffraction structures in the wing scales of *Callophrys rubi*, the Green Hairstreak. *J. Entomol. A* **49**, 149-152.
Nassau, K. (1983). *The Physics and Chemistry of Color.* New York: John Wiley & Sons.
Nijhout, H. F. (1991). *The Development and Evolution of Butterfly Wing Patterns.* Washington: Smithsonian Institution Press.
Otaki, J. M. and Yamamoto, H. (2004). Species-specific color-pattern modifications of butterfly wings. *Dev. Growth Differ.* **46**, 1-14.
Parker, A. R. (1999). Invertebrate structural colours. In *Functional Morphology of the Invertebrate Skeleton* (ed. E. Savazzi), pp. 65-90. London: John Wiley and Sons.
Prum, R. O. (2006). Anatomy, physics, and evolution of avian structural colors. In *Bird Coloration,* Vol. 1*, Mechanisms and Measurements* (ed. G. E. Hill and K. J. McGraw), pp. 295-353. Cambridge: Harvard University Press.
Prum, R. O. and Torres, R. H. (2003a). A Fourier tool for the analysis of coherent light scattering by bio-optical nanostructures. *Integr. Comp. Biol.* **43**, 591-602.
Prum, R. O. and Torres, R. H. (2003b). Structural colouration of avian skin: convergent evolution of coherently scattering dermal collagen arrays. *J. Exp. Biol.* **206**, 2409-2429.
Prum, R. O. and Torres, R. H. (2004). Structural colouration of mammalian skin: convergent evolution of coherently scattering dermal collagen arrays. *J. Exp. Biol.* **207**, 2157-2172.
Prum, R. O., Torres, R. H., Williamson, S. and Dyck, J. (1998). Coherent light scattering by blue feather barbs. *Nature* **396**, 28-29.
Prum, R. O., Torres, R. H., Kovach, C., Williamson, S. and Goodman, S. M. (1999a). Coherent light scattering by nanostructured collagen arrays in the caruncles of the *Malagasy asities* (Eurylaimidae: Aves). *J. Exp. Biol.* **202**, 3507-3522.
Prum, R. O., Torres, R. H., Williamson, S. and Dyck, J. (1999b). Two-dimensional Fourier analysis of the spongy medullary keratin of structurally coloured feather barbs. *Proc. R. Soc. Lond. B* **266**, 13-22.
Prum, R. O., Andersson, S. and Torres, R. H. (2003). Coherent scattering of ultraviolet light by avian feather barbs. *Auk* **120**, 163-170.
Prum, R. O., Cole, J. and Torres, R. H. (2004). Blue integumentary structural colours of dragonflies (Odonata) are not produced by incoherent Tyndall scattering. *J. Exp. Biol.* **207**, 3999-4009.
Soffer, B. H. and Lynch, D. K. (1999). Some paradoxes, errors, and resolutions concerning the spectral optimization of human vision. *Am. J. Phys.* **67**, 946-953.
Srinivasarao, M. (1999). Nano-optics in the biological world: beetles, butterflies, birds, and moths. *Chem. Rev.* **99**, 1935-1961.
Stavenga, D. G., Stowe, S., Siebke, K., Zeil, J. and Arikawa, K. (2004). Butterfly wing colours: scale beads make white pierid wings brighter. *Proc. R. Soc. Lond. B* **271**, 1577-1584.
Sweeney, A., Jiggins, C. and Johnsen, S. (2003). Polarized light as a butterfly mating signal. *Nature* **423**, 31-32.
van de Hulst, H. C. (1981). *Light Scattering by Small Particles.* New York: Dover.
Vukusic, P. and Sambles, J. R. (2000). Colour effects in bright butterflies. *J. Soc. Dyers Colourists* **116**, 376-380.
Vukusic, P. and Sambles, J. R. (2003). Photonic structures in biology. *Nature* **424**, 852-855.
Vukusic, P. and Hooper, I. (2005). Directionally controlled flourescence emission in butterflies. *Science* **310**, 1151.
Vukusic, P., Sambles, J. R., Lawrence, C. R. and Wooton, R. J. (1999). Quantified interference and diffraction in single *Morpho* butterfly scales. *Proc. R. Soc. Lond. B* **266**, 1403-1411.
Vukusic, P., Sambles, J. R. and Ghiradella, H. (2000a). Optical classification of microstructure in butterfly wing-scales. *Photon. Sci. News* **6**, 61-66.
Vukusic, P., Sambles, J. R. and Lawrence, C. R. (2000b). Structural colour: Colour mixing in wing scales of a butterfly. *Nature* **404**, 457.
Vukusic, P., Sambles, J. R., Lawrence, C. R. and Wakely, G. (2001a). Sculpted-multilayer optical effects in two species of *Papilo* butterfly. *Appl. Opt.* **40**, 1116-1125.
Vukusic, P., Sambles, J. R., Lawrence, C. R. and Wooton, R. J. (2001b). Now you see it – now you don't. *Nature* **410**, 36.
Vukusic, P., Sambles, J. R., Lawrence, C. R. and Wooton, R. J. (2002). Limited-view iridescence in the butterfly *Ancyluris meliboeus*. *Nature* **269**, 7-14.
Wickham, S., Large, M. C. J., Poladian, L. and Jermiin, L. S. (2005). Exaggeration and suppresion of iridescence: the evolution of two-dimensional butterfly structural colours. *J. R. Soc. Interface* **2**, doi:10.1098/rsif.2005.0071.
Yoshioka, S. and Kinoshita, S. (2003). Wavelength-selective and anisotropic light-diffusing scale on the wing of the *Morpho* butterfly. *Proc. R. Soc. Lond. B* **271**, 581-587.
Young, A. T. (1982). Rayleigh scattering. *Phys. Today* **35**, 42-48.